SLAC-PUB-12163
*BABAR*-PROC-06/100
hep-ex/0610049
October, 2006

# Study of Charm Baryons with the BaBar Experiment

B. Aa. Petersen
Stanford University
Stanford, California 94305, USA
(for the *BABAR* Collaboration)

**Abstract**

We report on several studies of charm baryon production and decays by the *BABAR* collaboration. We confirm previous observations of the $\Xi_c^{'0/+}$, $\Xi_c(2980)^+$ and $\Xi_c(3077)^+$ baryons, measure branching ratios for Cabibbo-suppressed $\Lambda_c^+$ decays and use baryon decays to study the properties of the light-quark baryons, $\Omega^-$ and $\Xi(1690)^0$.

Contributed to the Proceedings of the $33^{rd}$ International Conference on High Energy Physics, 7/26/2006—8/2/2006, Moscow, Russia

*Stanford Linear Accelerator Center, Stanford University, Stanford, CA 94309*

Work supported in part by Department of Energy contract DE-AC02-76SF00515.

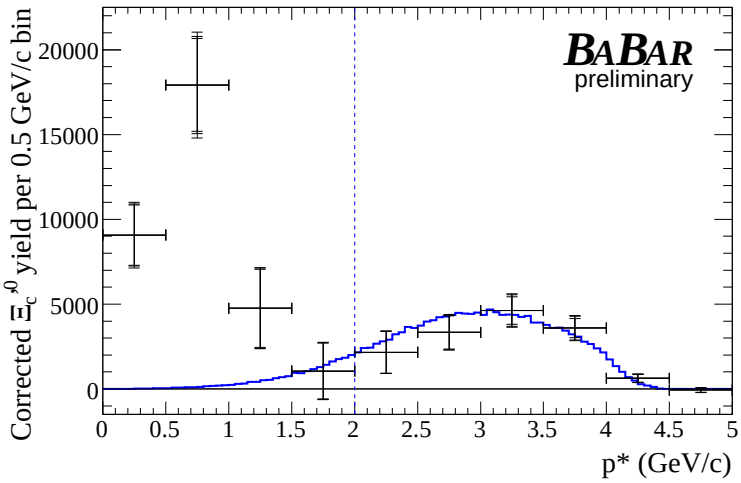


Figure 1: Efficiency-corrected, background-subtracted $p^*$ spectrum for $\Xi_c'^0$. The curve is the simulated continuum distribution; it is fitted to the data for $2.0 < p^* < 4.5\,\mathrm{GeV}/c$.

# 1 Introduction

The last few years have seen a revival of interest in charm spectroscopy with more than a dozen new states being reported and hundreds of new theoretical investigations being published. The *BABAR* experiment[1] provides excellent opportunities to observe and study new and old charm hadrons. It records $e^+e^-$ collisions at or just below the $\Upsilon(4S)$ resonance and with an integrated luminosity of $390\,\mathrm{fb}^{-1}$, the recorded data sample contains more than one billion charm hadron decays. About 10% of these are charm baryons and we report here on several charm baryon studies based on subsets of the *BABAR* data.

# 2 Production of $\Xi_c'$ Baryons

The isospin doublet $(\Xi_c'^0,\Xi_c'^+)$ was first observed by CLEO in $e^+e^-$ continuum events[2] and is identified as the lightest $J^P = \frac{1}{2}^+$ $csq$ baryon doublet with a symmetric light-quark wave-function. This observation has now been confirmed by *BABAR* and its production measured in both $e^+e^-$ continuum events and $B$ decays.[3]

The *BABAR* analysis uses $232\,\mathrm{fb}^{-1}$ of data. The $\Xi_c'^{0(+)}$ baryon is reconstructed in the only kinematically allowed decay mode: $\Xi_c'^{0(+)} \to \Xi_c^{0(+)}\gamma$. The $\Xi_c^{0(+)}$ is reconstructed from the decay chain, $\Xi_c^{0(+)} \to \Xi^-\pi^+(\pi^+)$, $\Xi^- \to \Lambda\pi^-$, $\Lambda \to p\pi^-$. Clear signals for $\Xi_c'^{0(+)}$ are observed in the $\Xi_c^{0(+)}\gamma$ invariant mass spectrum and yields are extracted from fits to the mass spectrum in $0.5\,\mathrm{GeV}/c$ wide bins of $p^*$, the $\Xi_c'^{0(+)}$ momentum in the $e^+e^-$ center-of-mass frame. The results for $\Xi_c'^0$ are shown in Fig. 1 after correcting for reconstruction efficiency. $\Xi_c'^{0(+)}$ baryons with $p^* > 2\,\mathrm{GeV}/c$ come from continuum production, while most baryons with $p^* < 2\,\mathrm{GeV}/c$ are due to $B$ decays. Using a model of $\Xi_c'^{0(+)}$ continuum production, the yield for $p^* > 2\,\mathrm{GeV}/c$ is extrapolated to the full $p^*$ range. From this the $B$ component is separated to obtain the branching fractions $\mathcal{B}(B \to \Xi_c'^+X) \times \mathcal{B}(\Xi_c^+ \to \Xi^-\pi^+\pi^+) = [1.69 \pm 0.17\ (\mathrm{exp.}) \pm 0.10\ (\mathrm{model})] \times 10^{-4}$ and $\mathcal{B}(B \to$

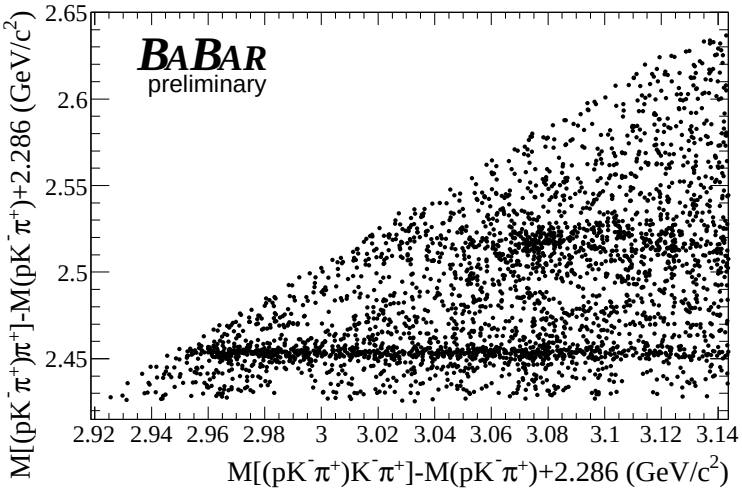


Figure 2: Two-dimensional scatter plot of $M(\Lambda_c^+\pi^+)$ vs. $M(\Lambda_c^+K^-\pi^+)$ for $pK^-\pi^+K^-\pi^+$ candidates.

$\Xi_c^{\prime 0}X)\times\mathcal{B}(\Xi_c^0\to\Xi^-\pi^+)=[0.67\pm0.07\ (\mathrm{exp.})\pm0.03\ (\mathrm{model})]\times10^{-4}$. This is the first observation of the $\Xi_c^{\prime}$ baryon in $B$ decays. The measured continuum production cross sections are $\sigma(e^+e^-\to\Xi_c^{\prime +}X)\times\mathcal{B}(\Xi_c^+\to\Xi^-\pi^+\pi^+)=141\pm24\ (\mathrm{exp.})\pm19\ (\mathrm{model})$ fb and $\sigma(e^+e^-\to\Xi_c^{\prime 0}X)\times\mathcal{B}(\Xi_c^0\to\Xi^-\pi^+)=70\pm11\ (\mathrm{exp.})\pm6\ (\mathrm{model})$ fb. Comparing to a previous measurement of $\Xi_c^0$ production,[4] one observes that about one third of the $\Xi_c^0$ produced in $B$ decays come from $\Xi_c^{\prime 0}$ decays, while in continuum the fraction is only 18%.

## 3 $\Xi_c(2980)^+$ and $\Xi_c(3077)^+$

Two new charm-strange baryons, $\Xi_c(2980)^+$ and $\Xi_c(3077)^+$, were recently observed by BELLE in decays to $\Lambda_c^+K^-\pi^+$.[5] These are the first baryon decays where the charm and strange quark are contained in separate hadrons. *BABAR* has confirmed this observation and studied the resonant substructure in the decay.[6]

For this study *BABAR* uses $316\,\mathrm{fb}^{-1}$ of data. The $\Lambda_c^+$ baryons are reconstructed in the decay mode $\Lambda_c^+\to pK^-\pi^+$ and combined with a second kaon and pion candidate. The invariant mass of the $\Lambda_c^+\pi^+$ pair are plotted versus the mass of the $\Lambda_c^+K^-\pi^+$ candidate in Fig. 2. Horizontal bands from the $\Sigma_c(2520)^{++}$ and $\Sigma_c(2455)^{++}$ resonances are observed and enhancements around 2970 and $3077\,\mathrm{MeV}/c^2$ in $M(\Lambda_c^+K^-\pi^+)$ can also be seen.

To extract the yields of the $\Xi_c(2980)^+$ and $\Xi_c(3077)^+$ baryons and determine how much decays through a $\Sigma_c^{++}$ resonance, a two-dimensional unbinned likelihood fit is performed on the events shown in Fig. 2. The fit contains both resonant $\Sigma_c^{++}$ components and non-resonant components for both the $\Xi_c(2980)^+$ and $\Xi_c(3077)^+$ signals and the background. Phase-space suppression factors are including in the signal PDFs to account for the nearby kinematic thresholds.

The fitted PDF is overlaid on the data in Fig. 3 and the fit yields are given in Table 1. The statistical significance of both the $\Xi_c(2980)^+$ and the $\Xi_c(3077)^+$ signals exceed $7\,\sigma$. The $\Sigma_c^{++}$ resonances are seen to be dominant in the $\Xi_c(3077)^+$ decay, while only about 50% of the $\Xi_c(2980)^+$ decays are through $\Sigma_c(2455)^{++}$. The mass and width of the two resonances are also obtained in

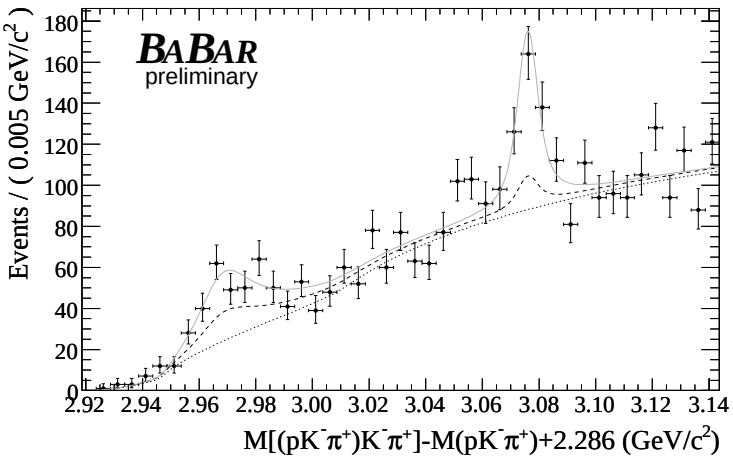


Figure 3: Invariant mass distribution of $\Lambda_c^+ K^-\pi^+$ for data (points with error bars) and the fitted PDF (curves). The solid curve shows the total fit PDF. The dotted curve shows the sum of the background components, while the dashed curve on top shows the sum of the non-resonant signal components.

Table 1: Yields for the separate resonant and non-resonant (NR) decays.

| | Yield (Events) |
|---|---|
| $\Xi_c(2980)^+ \to \Sigma_c(2455)^{++}K^-$ | $132 \pm 31 \pm 5$ |
| $\Xi_c(2980)^+ \to \Lambda_c^+ K^-\pi^+$ (NR) | $152 \pm 37 \pm 45$ |
| $\Xi_c(3077)^+ \to \Sigma_c(2455)^{++}K^-$ | $87 \pm 20 \pm 4$ |
| $\Xi_c(3077)^+ \to \Sigma_c(2520)^{++}K^-$ | $82 \pm 23 \pm 6$ |
| $\Xi_c(3077)^+ \to \Lambda_c^+ K^-\pi^+$ (NR) | $35 \pm 24 \pm 16$ |

Table 2: Comparison of masses and widths for $\Xi_c(2980)^+$ and $\Xi_c(3077)^+$, measured by *BABAR* and BELLE in the $\Lambda_c^+ K^-\pi^+$ final state.

| | Mass ( MeV/$c^2$) | Width ( MeV) |
|---|---|---|
| *BABAR* | $2967.1 \pm 1.9 \pm 1.0$ | $23.6 \pm 2.8 \pm 1.3$ |
| BELLE | $2978.5 \pm 2.1 \pm 2.0$ | $43.5 \pm 7.5 \pm 7.0$ |
| *BABAR* | $3076.4 \pm 0.7 \pm 0.3$ | $6.2 \pm 1.6 \pm 0.5$ |
| BELLE | $3076.7 \pm 0.9 \pm 0.5$ | $6.2 \pm 1.2 \pm 0.8$ |

the fit and are compared to the results from BELLE in Table 2. The parameters for the $\Xi_c(3077)^+$ baryon agree, but for the $\Xi_c(2980)^+$ the *BABAR* mass and width are lower. This might be due to different treatment of the phase-space suppression.

## 4 Cabibbo-Suppressed $\Lambda_c^+$ Decays

Only a few Cabibbo-suppressed $\Lambda_c^+$ decays have been measured and most have poor precision. *BABAR* has performed a precise measurement of two Cabibbo-suppressed decay modes and searched for two new decays.[7]

The analysis uses $125\,\mathrm{fb}^{-1}$ of data. It combines $\Lambda$ and $\Sigma^0$ candidates with $K^+$ candidates to reconstruct $\Lambda_c^+ \to \Lambda K^+$ and $\Lambda_c^+ \to \Sigma^0 K^+$ decays. Large signals are seen in both decay modes and used together with signals from the Cabibbo-favored $\Lambda_c^+ \to \Lambda\pi^+$ and $\Lambda_c^+ \to \Sigma^0\pi^+$ decays to obtain the branching ratios:

$$\begin{aligned}
\frac{\mathcal{B}(\Lambda_c^+ \to \Lambda K^+)}{\mathcal{B}(\Lambda_c^+ \to \Lambda\pi^+)} &= 0.044 \pm 0.004 \pm 0.003, \\
\frac{\mathcal{B}(\Lambda_c^+ \to \Sigma^0 K^+)}{\mathcal{B}(\Lambda_c^+ \to \Sigma^0\pi^+)} &= 0.039 \pm 0.005 \pm 0.003,
\end{aligned}$$

where the first uncertainty is statistical and the second systematic. These are a significant improvement over previous measurements[8] and in agreement with quark-model predictions.[9]

Searches for the four-body decays $\Lambda_c^+ \to \Lambda K^+\pi^+\pi^-$ and $\Lambda_c^+ \to \Sigma^0 K^+\pi^+\pi^-$ are also performed. After removing decays with intermediate resonances ($\Lambda K^+ K_S^0$ and $\Xi^- K^+\pi^+$), no significant signals are observed and the following upper limits at 90% confidence level are obtained:

$$\begin{aligned}
\frac{\mathcal{B}(\Lambda_c^+ \to \Lambda K^+\pi^+\pi^-)}{\mathcal{B}(\Lambda_c^+ \to \Lambda\pi^+)} &< 4.1 \times 10^{-2}, \\
\frac{\mathcal{B}(\Lambda_c^+ \to \Sigma^0 K^+\pi^+\pi^-)}{\mathcal{B}(\Lambda_c^+ \to \Sigma^0\pi^+)} &< 2.0 \times 10^{-2}.
\end{aligned}$$

The measurements are the first limits on these decay modes.

## 5 Measurement of the $\Omega^-$ Spin

The quark model successfully predicted[10] the existence of the $\Omega^-$ baryon. It also predicts its spin to be 3/2, but until now experiments have only established that its spin is larger than 1/2. *BABAR* has studied its spin by using $\Xi_c^0 \to \Omega^-\pi^+, \Omega^- \to \Lambda K^-$ decays reconstructed in $116\,\mathrm{fb}^{-1}$ of data.[11] The distribution of the helicity angle $\theta_h$, defined as the angle between the $\Lambda$ and the $\Xi_c^0$ in the $\Omega^-$ rest-frame, depends on the spin $J$ of the $\Omega^-$ and the $\Xi_c^0$. Assuming $J_{\Xi_c^0} = 1/2$, the distributions for $J_\Omega = 1/2$, 3/2 and 5/2, respectively are:

$$dN/d\cos\theta_h \propto 1 \tag{1}$$

$$dN/d\cos\theta_h \propto 1 + 3\cos^2\theta_h \tag{2}$$

$$dN/d\cos\theta_h \propto 1 - 2\cos^2\theta_h + 5\cos^4\theta_h \tag{3}$$

Parity violation in the $\Xi_c^0$ and $\Omega^-$ decays could give an additional term with odd powers of $\cos\theta_h$, but no evidence for that is seen in data.

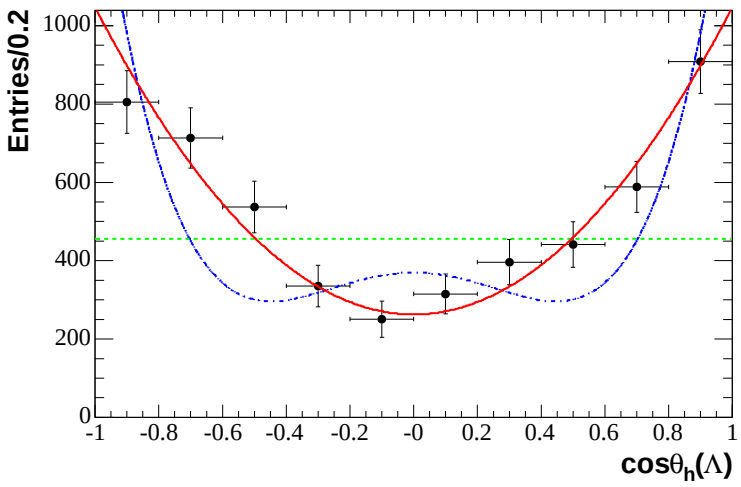


Figure 4: The efficiency-corrected $\cos\theta_h(\Lambda)$ distribution for $\Xi_c^0 \to \Omega^- K^+$ data. The curves represents the expected distribution for $J_\Omega = 1/2$ (dashed), $J_\Omega = 3/2$ (solid) and $J_\Omega = 5/2$ (dashed-dotted).

Figure 4 shows the helicity angle distribution with the three spin hypothesis overlaid. The $J_\Omega = 3/2$ hypothesis is in clear agreement with data, while the confidence levels for the $J_\Omega = 1/2$ and $J_\Omega = 5/2$ hypotheses are $1 \times 10^{-17}$ and $3 \times 10^{-7}$, respectively. This confirms that the $\Omega^-$ baryon has the expected spin.

## 6 Study of the $\Xi(1690)^0$ Baryon

The existence of the $\Xi(1690)^0$ baryon has been known for many years, but relatively little information is available on it. BELLE has observed it as an intermediate resonance in $\Lambda_c \to (\Lambda K_S^0)K^+$ decays.[8] *BABAR* uses this decay mode in a larger data sample ($200\,\mathrm{fb}^{-1}$) to measure the mass, width and spin of the $\Xi(1690)^0$ baryon.[12]

*BABAR* reconstructs $2750 \pm 300$ $\Lambda_c \to \Lambda K_S^0 K^+$ decays and the $\Xi(1690)^0$ is clearly visible in invariant mass of the $\Lambda K_S^0$ pair (see Fig. 5). The remaining $\Lambda_c^+$ decays cannot be described as a non-resonant contribution. Instead they appear to be decays through $\Lambda a_0(980)^+$, where $a_0(980)^+ \to K_S^0 K^+$. To measure the mass and width of the $\Xi(1690)^0$, the mass projections of the $\Lambda K_S^0 K^+$ Dalitz plot are fitted to a coherent sum of $\Lambda a_0(980)^+$ and $\Xi(1690)^0 K^+$ decays. The fit result is overlaid in Fig. 5 and gives

$$\begin{aligned} m(\Xi(1690)) &= 1684.7 \pm 1.3\,^{+2.2}_{-1.6}\,\mathrm{MeV}/c^2, \\ \Gamma(\Xi(1690)) &= 8.1^{+3.9}_{-3.5}\,^{+1.0}_{-0.9}\,\mathrm{MeV}, \end{aligned}$$

where the first uncertainty is statistical and the second systematic, primarily related to the interference contribution. Both the mass and the width measurements are significant improvements over previous results.

The spin of the $\Xi(1690)^0$ baryon can be studied analogously to the $\Omega^-$ spin. Assuming the $\Lambda_c^+$ baryon has spin 1/2, the $\Xi(1690)^0$ is found to be fully consistent with spin 1/2, while the spin 3/2

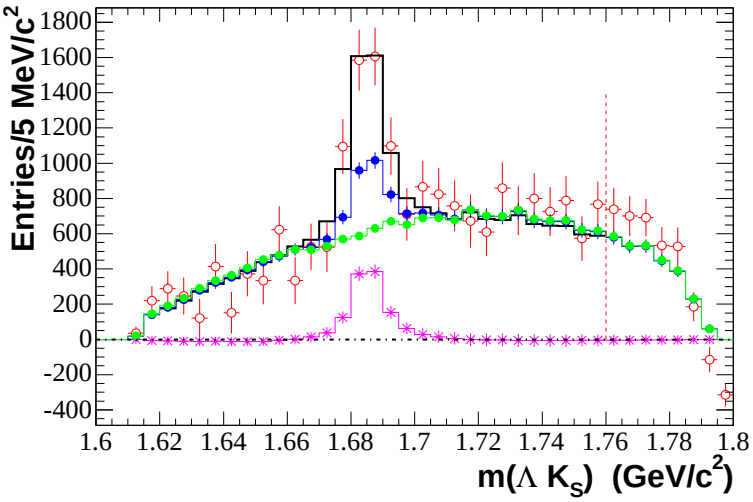


Figure 5: The $\Lambda K_S$ invariant mass projection in data (open circles) with the fit overlaid (black line). Superimposed is the distribution for the $\Lambda a_0(980)^+$ contribution (light-colored dots), the interference term (stars) and their sum (dark-colored dots).

and 5/2 hypotheses only have confidence levels of 0.02 and 0.01, respectively. This is the first spin measurement for the $\Xi(1690)^0$ baryon.

## 7 Summary

The large sample of charm hadrons recorded by the *BABAR* experiment has been used to study the properties of several charm baryons. Furthermore, the decays of charm baryons are used as a clean source of light-quark baryons whose spin, mass and width are measured.

## References


[1] B. Aubert *et al.*, *Nucl. Instr. Methods Phys. Res., Sect. A* **479**, 1 (2002).

[2] C. P. Jessop *et al.*, *Phys. Rev. Lett.* **82**, 492 (1999).

[3] B. Aubert *et al.*, hep-ex/0607086.

[4] B. Aubert *et al.*, *Phys. Rev. Lett.* **95**, 142003 (2005).

[5] R. Chistov *et al.*, Submitted to *Phys. Rev. Lett.*, hep-ex/0606051.

[6] B. Aubert *et al.*, hep-ex/0607042.

[7] B. Aubert *et al.*, Submitted to *Phys. Rev. D.*, hep-ex/0601017.

[8] K. Abe *et al.*, *Phys. Lett.* **B524**, 33 (2002).

[9] T. Utpal, R. C. Verma and M. P. Khana, *Phys. Rev.* **D49**, 3417 (1994).

[10] M. Gell-Mann, Proceedings of the International Conference on High-Energy Physics, p. 805 (1962).

[11] B. Aubert *et al.*, *Phys. Rev. Lett.* **97**, 112001 (2006).

[12] B. Aubert *et al.*, hep-ex/0607043.